Journal of Robotics and Control (JRC)
Volume 6, Issue 2, 2025
ISSN: 2715-5072, DOI: 10.18196/jrc.v6i2.25763

Comparison of Adaptive Sliding Mode Controllers in Earthquake Induced Vibrations

Alaa Al-Tamimi [1*], T. MohammadRidha [2]
[1, 2] Control and Systems Engineering Department, University of Technology - Iraq, Baghdad 10066, Iraq
Email: [1] cse.22.13@grad.uotechnology.edu.iq, [2] taghreed.m.ridha@uotechnology.edu.iq
*Corresponding Author

***Abstract*—This study aims to reduce earthquake-related vibrations in buildings. This is achieved by designing two different robust adaptive control algorithms to control the damping force of the dampers. This design is used in mitigating the structural vibrations of a three-story prototype building exposed to two different scaled earthquakes. Two cases are considered where two damping systems are employed and mounted on the top floor: an Active Tuned Mass Damper (ATMD), the second damper is a semi-active Magnetorheological Damper (MRD). The first damper depends entirely on the control algorithm to correct structural movement; the second one operates as a passive damper under minor vibrations and becomes active under stronger vibrations. The results showed that one of the adaptive algorithms give a better displacement reduction and error indices across all floors. Furthermore, integrating that controller with MRD demonstrated higher accuracy in tracking the structural response with less control effort compared to ATMD. To validate the method effectiveness, it was compared to another robust sliding mode controller from the literature. The results show a significant improvement in displacement reduction and less control effort by 40.23% better than the control effort of the previous work. These findings highlight the potential of combining advanced control strategies with semi-active damping systems for effective vibration mitigation and energy efficiency.**

Keywords*—*Adaptive Sliding Mode Control; MR-Damper; ATMD-Damper; Building Vibration; Earthquakes.

I. INTRODUCTION

In 2024, the world witnessed numerous devastating earthquakes, including the Noto Peninsula earthquake in Japan, which resulted in significant loss of life and economic damage [1]-[3]. Earthquakes occur suddenly and pose serious risks to structures and human safety. To mitigate these risks, dampers are added to buildings to reduce vibrations and minimize their impact. These dampers are devices that come in various types, including passive, active, and semi-active. Unlike passive dampers, active and semi-active dampers incorporate control algorithms designed to enhance their efficiency in absorbing seismic energy. Researchers have focused on developing advanced control strategies to optimize the performance of these dampers, ensuring the safety of both human life and infrastructure [4]-[6]. The different types of dampers vary in their operation and effectiveness. For example, passive dampers, which absorb seismic energy, are one strategy for reducing structural vibrations [6]-[11]. However, these dampers lack feedback signals and thus are insufficient [12]-[14]. To address this, active dampers were developed, which operate through an external power source controlled by an algorithm. The control signal is generated based on feedback measurements of the structural state variables. Active dampers, such as the Active Tuned Mass Damper (ATMD), are effective in mitigating vibrations but suffer from the need for a high-power source [15]-[17]. Consequently, semi-active control has emerged as an alternative, offering solutions that require less energy, such as Magnetorheological Dampers (MRD), which can track the movement of the structure in real time [18]-[23] operating using battery power [24]. These dampers contain a specialized fluid that quickly transitions from a liquid to a semi-solid state within seconds when exposed to a magnetic or electric field [25]-[28].

Many studies in this field aim to design robust and efficient control algorithms for both active and semi-active dampers [29]-[37]. In recent years, several studies have been conducted to explore the effects of earthquakes on buildings, whether single-story or multi-story, with the aim of developing effective control systems to reduce vibrations caused by earthquakes. In a study on single-story buildings, Hamidi et al. [38] applied an Adaptive Backstepping Sliding Mode Control (ABSMC) system using MRD. The results showed that the ABSMC system consumes more energy compared to the traditional sliding mode control (SMC), but it was necessary to achieve the desired displacement. However, this system requires prior knowledge of disturbance boundaries, which may limit its application in some cases. As for multi-story buildings, several studies have been conducted such as Yan et al. [39] who used three control algorithms with different dampers to evaluate the effectiveness of the ATMD device for mitigating earthquake-induced vibrations in a ten-story structure. The employed algorithms comprised a conventional TMD, Linear Quadratic Regulator (LQR) and Fuzzy Neural Network (FNN). The results indicated LQR system achieved a 70.77% enhancement in reducing displacement, but the TMD demonstrated less effectiveness. Conversely, the FNN algorithm shown efficiency as an alternative, achieving comparable results without necessitating a precise mathematical model. Khatibinia et al. [40] developed an Optimal Sliding Mode Control (OSMC) system to control an 11-story building equipped with ATMD on the top floor. The performance of OSMC was compared with other control systems such as PID, LQR, and Fuzzy Logic Controller (FLC) during simulated seismic events. The results showed that OSMC reduced displacement by an additional 36.7% compared to other systems. Wasilewski et al. [41] developed an adaptive optimal control system for a 20-story structure equipped with an Active Tuned Mass Damper (ATMD). The research evaluated three categories of control systems: Linear-Quadratic-Gaussian (LQG), H∞, and adaptive optimal control. The systems were testing through various seismic simulations, including the Kobe and El Centro earthquakes. The results showed that the adaptive control system significantly outperformed conventional methods, reducing acceleration drift by as much as 50%. Li et al. [42] proposed Model Reference Sliding Mode Control (MRSMC) and Unscented Kalman Filter (UKF) to determine unknown states and parameters in real time for a 3-story building equipped with an Active Mass Damper (AMD) placed on the top floor to reduce nonlinear vibrations during seismic events. The results showed significant improvement, with the maximum displacement of the third floor reduced by 70.77%, Story displacement reduced by 78.05% and 61.67%, and the maximum acceleration of the third floor reduced by 67.22%. There is a well-known case study of a 3-story prototype building exposed to scaled simulated earthquakes; the related research to this case are presented in what follows. Jagadisha et al. [43] developed a PID controller with MRD to improve the building's response to earthquakes. The damper was installed on the first floor, and the system was tested under the impact of El Centro, Northridge, and Kobe earthquakes. The results showed significant improvement in reducing displacement, with the maximum displacement reduced by 30–40%. Zizouni et al. [44], proposed a LQR system with MRD to reduce earthquake-induced vibrations. The damper was installed on the first floor, and the system was tested under the impact of the El Centro1940 earthquake. The results showed a significant reduction in displacement, with the maximum displacement reduced by up to 40% on the first floor and 30-35% on the upper floors. In another study Zizouni et al. [45], proposed neural network to control MRD for reducing earthquake-induced vibrations in a 3-story building was proposed. The damper was installed between the ground floor and the first floor, and the system was tested under the impact of Tohoku and Boumerdès 2003 earthquakes. The results showed significant improvement in reducing displacement, with reduction rates ranging from 57.64% to 72.20%. Saidi et al. [46] proposed Adaptive Sliding Mode Control (ASMC) equipped with MRD on the ground floor of this 3-story building to reduce earthquake-induced vibrations. The system was tested under the impact of the El Centro1940 and 2003 Boumerdès earthquakes. The results showed significant improvement in reducing of displacement by 60.1% during the El Centro1940 and 50.4% during the Boumerdès. In another study by Zizouni et al. [47], MRD was used on the ground floor of the 3-story building with ASMC. The system was tested under the impact of the El Centro 1940 earthquake. The results showed significant improvement in reducing displacement, with displacement reduced by 78.05% on the first floor, 73.87% on the second floor, and 69.92% on the third floor. Finally, Husain and MohammadRidha [48], proposed Integral Sliding Mode Control using a barrier function (ISMCb) equipped with MRD placed on the top floor of the 3-story building. The performance of MRD was compared with ATMD under the impact of the Mexico City and El Centro1940 earthquakes. The results showed that MRD outperformed ATMD in reducing displacement, achieving improvements of 83.9% during the Mexico City earthquake and 76% during the El Centro 1940 earthquake. These studies show continuous progress in the control systems used to reduce earthquake-induced vibrations.

The aim of this study is to reduce building vibrations due to earthquakes and to reduce the required control effort as well. This is achieved by the design of adaptive sliding mode control to command the behavior of damping devices. The three-story building case study is considered for the following control system design tests under different earthquake excitations:

1. A new adaptive approach (ASMC1) developed in [49], [50] is designed with an ATMD. Its performance is compared to ASMC2 performance from [47] showing that ASMC2 has a better displacement reduction
2. ASMC2 design in [47] is modified here and the MRD is placed on top floor unlike in [47] where it was placed on the ground floor. the comparation showed a better displacement reduction is achieved when MRD is on top floor
3. The final modified design of ASMC2 is compared to ISMCb from the literature [48].The results showed a better performance is achieved using proposed ASMC2.

This paper is structured as follows: Section 2 presents the mathematical model of a building including ATMD and MRD. The ASMC algorithms are explained in Section 3. Section 4 result and discussed. The conclusion is presented in Section 5.

II. Mathematical Model

The system studied in this research consists of a three-story building prototype equipped with a damper on the top floor to absorb vibrations caused by earthquakes. The dynamics of the building is given below [51], [52]:

$$M\ddot{x}(t) + C\dot{x}(t) + K(t) = M\Lambda\ \ddot{x}_g(t) - Pf_D \tag{1}$$

where $x, \dot{x}, and\ \ddot{x}$ are displacement, velocity and acceleration vectors of the structure respectively. $x = [x_1, x_2, x_3, \dots, x_n]^T$, where n is the number of floors and in this work n=3. $C, K\ and\ M \in R^{n*n}$ are damping, stiffness and mass matrices. $\ddot{x}_g$ is the unknown earthquake acceleration. $\Lambda \in R^{n*1}$ is unity vector, f_D is the force produced by the dampers, $P \in R^{n*1}$ represents the location of each damper. In this work the damper is located in the top floor and only one damper will be considered, hence:

$$P = [0, 0, 0, 0, 0, 1]^T \tag{2}$$

State equation representation for (1) is as follows:

$$\dot{x} = Ax + Bf_D + D\ddot{x}_g \tag{3}$$

where, $B\ and\ D$ are $\in R^{2n*1}$, $A \in R^{2n*2n}$, f_D is the damper force. The matrices are represented as follows:

$$A = \begin{bmatrix} 0 & I \\ -M^{-1}K & -M^{-1}C \end{bmatrix}, B = \begin{bmatrix} 0 \\ -M^{-1}P \end{bmatrix}, D = \begin{bmatrix} 0 \\ -\Lambda \end{bmatrix} \tag{4}$$

$$\ddot{x}_g| \leq \delta \tag{5}$$

The acceleration of the earthquake in this work is assumed to be bounded, with δ representing the upper bound of the unknown earthquake. In the next subsection, the damping systems employed here: ATMD and MRD models are presented.

A. *Mathematical Model for ATMD*

ATMD is active tuned mass damper located on the top floor of a three-story building. Its principle of generated forces opposes the seismic forces operating on the structure [53]. Fig. 1 illustrates the relationship between the damper, the building, and the control signal.

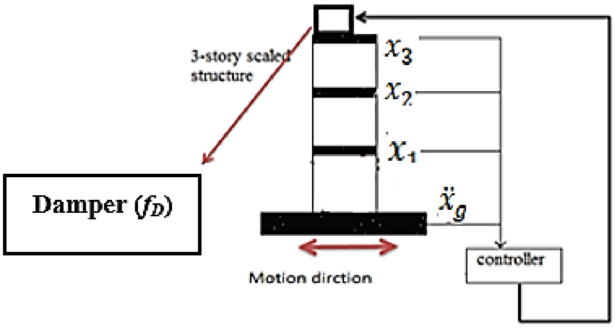

Fig. 1. The system's schematic [48], [54]

The mathematical model of ATMD is represented below [55]:

$$m_d\left(\ddot{x}_d(t)+\ddot{x}_n(t)+\ddot{x}_g(t)\right)=f_D(t) \tag{6}$$

$$f_D(t)=u-k_d x_d(t)-c_d\dot{x}_d(t) \tag{7}$$

The variables m_d, k_d, and c_d represent ATMD mass, stiffness, and damping, respectively. u is the control signal applied to the ATMD, while $f_D(t)$ represents the net force acting on ATMD. $\ddot{x}_n(t)$ represents the top floor's acceleration.

B. *Mathematical Model for MRD*:

The MRD seen in Fig. 2 is a semi-active damper includes a hydraulic cylinder, divided by a piston head. The cylinder contains a fluid with special characteristics (viscous fluid) that can pass through narrow orifices. The two sides of the cylinder connect by an external valve that regulates the operation of the device. The semi-active stiffness control device changes the system dynamics by adjusting the structural stiffness [38]. Furthermore, it is driven by a small battery, as it requires less than 50 Watts of power. Additionally, the MRD responds in milliseconds and operates within a temperature range of -40℃ to +150℃ [38]. MRD is commonly used for seismic control due to the simplicity of installation and maintenance, as well as its compact size, allowing installation on any floor of the building. The nonlinear model of MRD which described by the modified Bouc–Wen model, this model was presented by [55]. The applied force suggested by this model is governed as follow:

$$f_D = c_1\dot{y} + k_0\,(x - y) + k_1\,(x - x_1)\alpha z \tag{8}$$

$$\dot{y} = \frac{1}{c_0+c_1}(c_0\,\dot{x} + k_0(x - y) + \alpha z) \tag{9}$$

$$\dot{z} = -\Upsilon|\dot{x} - \dot{y}|z|z|^{r-1} - \beta(\dot{x} - \dot{y})|z|^r + a(\dot{x} - \dot{y}) \tag{10}$$

where, x and $\dot{x}$, are taken from the floor where the damper is mounted respectively, f_D, z, k_0 and k_1 are generated force, hysteretic component, accumulator stiffness respectively at low and high velocity. Υ, β, r and a are parameters giving the shape and scale of the hysteresis loop. c_0 and c_1 are the viscous damping at low and high velocity respectively, which depend on control voltage as seen in Eq. (11), (12), (13) and (14) respectively:

$$\alpha = \alpha_a + \alpha_b\mu \tag{11}$$

$$c_1 = c_{1a} + c_{1b}\mu \tag{12}$$

$$c_0 = c_{0a} + c_{0b}\,\mu \tag{13}$$

$$\dot{\mu} = -F_t(\mu - vc) \tag{14}$$

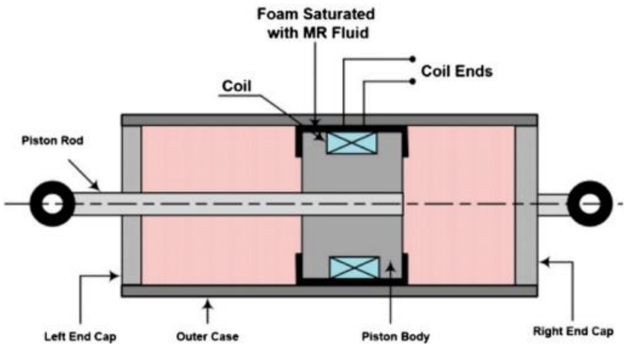

Fig. 2. Schematic representation of MR damper [38]

In (14), F_t represents time response factor, μ is a phenomenological variable enveloping the system, and v_c is the command voltage applied to the damper's control circuit. The resulting provided control voltage of MRD is shown below [46], [55]-[57]:

$$v_c = v_{max}H[(u - f_D(t)).f_D(t)] \tag{15}$$

where v_{max} is the maximum applied voltage and the range from 0 to *2.25volt*, *u* is the controller signal (control algorithm), and $f_D(t)$ the force created by damper. $H(.)$ represents a Heaviside step function.

The next section presents the methodology for the control algorithm to drive the dampers: u.

III. Adaptive Sliding Mode Controller Design

Sliding mode control (SMC) is a robust control that rejects matched perturbations, making it commonly employed due to its favored robust performance [51], [55], [56], [58]-[61]. SMC comprises two phases: the reaching phase and the sliding phase. Perturbation affects the system during the reaching phase but not during the sliding phase SMC requires knowledge of the boundaries of disturbances and uncertainties [62]. One of the challenges in SMC is the chattering caused by the rapid switching of the discontinuous function. Adding an adaptive mechanism can improve the controller's response, and undesirable chattering can be reduced [49].Take the following example of the system state dynamics described by:

$$\dot{x} = f(x,t) + g(x,t).u(x) \tag{16}$$

Where $x \in \mathrm{R}^N$ the state is vector, $f(x,t) \in R^{N\times N}$ *and* $g(x,t) \in R^{N\times m}$ are nonlinear functions furthermore, $f(x,t)$ contains unmeasured perturbations, and $u \in R^m$ is the control law. The sliding variable s is given by:

$$s(x.t) = \bar{G}\,x \tag{17}$$

Where, $\bar{G} = [\bar{g}_1\ \bar{g}_2\ \dots \bar{g}_N\ ]$ to be designed. The dynamics of the sliding variable is:

$$\dot{s} = \frac{\partial s}{\partial x}\dot{x} + \frac{\partial s}{\partial t} = \frac{\partial s}{\partial x}(f(x) + gu) + \frac{\partial s}{\partial t} \tag{18}$$

$$= \left(\frac{\partial s}{\partial t} + \frac{\partial s}{\partial x}\ f(x)\right) + \left(\frac{\partial s}{\partial x}\ gu\right) \tag{19}$$

$$\dot{s} = \Psi(x.t) + \Gamma(x.t) \cdot u \tag{20}$$

Ψ and Γ are bounded functions but their upper bounds are $|\Psi| \le \Psi_M$ and $0 < \Gamma_m \le \Gamma \le \Gamma_M$. According to CSMC, the design of discontinuous control is:

$$u = -k\ sign(s) \tag{21}$$

The value of k is chosen through a candidate Lyapunov function.

$$V(s) = \frac{1}{2}\ s^2 \tag{22}$$

The derivative is as follows:

$$\dot{V}(s) = s\ \dot{s} = s(\Psi(x.t) + \Gamma(x.t) \cdot u) \tag{23}$$

$$\dot{V}(s) \le |s|(\ |\Psi| - |\Gamma| \cdot k) < 0 \tag{24}$$

$$k \ge \left|\frac{\Psi_M}{\Gamma_m}\right| \tag{25}$$

The control gain K is fixed and has a significant value to overcome the upper bound of the perturbation that can face the system, which leads to the high amplitude chattering phenomenon. Also, the upper bounds of uncertainties/ perturbations are needed to determine its value. One solution for these issues is adopting the Adaptive Sliding Mode Control (ASMC) approaches [49].

The use of ASMC continues to expand across a wide range of systems, playing a fundamental role in enhancing the performance of structures subjected to seismic excitations [38], [46], [63], [64]. Controlling such structures requires addressing multiple challenges, particularly mitigating the impact of external disturbances that affect their stability and dynamic response.In this context, this section examines two adaptive sliding mode control algorithms: ASMC1 and ASMC2. The first algorithm (ASMC1) is based on the equivalent control principle, which reduces the control gain; however, it requires knowledge of the disturbance bounds [49]. To solve this problem we used the second algorithim [47]. In what follows, ASMC1 and ASMC2 design principles are illustrated.

A. First Adaptive Sliding Mode Controller (ASMC1)

In this section, ASMC1 is designed for the first time for the system in Eq. (3) equipped with ATMD in Eq. (6) and (7). Firstly, the design of the sliding manifold is defined $\bar{G} = [\bar{g}_1\ \bar{g}_2\ \bar{g}_3\ \bar{g}_4\ \bar{g}_5\ \bar{g}_6\ ]$ and it is designed such that $\Gamma = \bar{G}B$ is nonsingular square matrix and the closed-loop system dynamics is stable. Eq. (26) provides the derivative of the sliding manifold to examine the sliding mode dynamics:

$$\dot{s} = \bar{G}\dot{x} = \bar{G}\,(A\,x + Bf_D + D\,\ddot{x}_g\,) \tag{26}$$

To ensure reachability of the sliding manifold, the candidate Lyapunov function can be described as:

$$V = \frac{1}{2}s^2 \tag{27}$$

The time derivative of the Lyapunov Function gives:

$$\dot{V} = s\dot{s} \tag{28}$$

Substituting Eq. (26) in Eq. (28) we get:

$$\dot{V} = s(\bar{G}Ax + \Gamma f_D + \bar{G}D\ \ddot{x}_g \tag{29}$$

$$f_D = u - k_d x_d - c_d \dot{x}_d \tag{30}$$

Select the control low as:

$$u = -(\Gamma)^{-1}k(t)\ sign(s) \tag{31}$$

Substituting Eq. (31) in (30) then in Eq. (29) results:

$$\dot{V} = s(\bar{G}Ax + \Gamma(-(\Gamma)^{-1}k\ sign(s) - k_d x_d - c_d\dot{x}_d\ ) + \bar{G}D\ \ddot{x}_g) \tag{32}$$

Define:

$$\Psi = \bar{G}Ax\ - \Gamma(k_d x_d + c_d\dot{x}_d) + \bar{G}D\ \ddot{x}_g \tag{33}$$

$$|\Psi| \le \ \Psi_{max} \tag{34}$$

where f_D is a force of damper ATMD and taking the upper bounds in (5), (34) yields:

$$\dot{V} \le -|s|[k - \Psi_{max}] \tag{35}$$

k is a positive switching gain, will be designed next, Choose k such that $\dot{V}$ is negative definite to ensure the sliding manifold attractiveness:

$$k \ge \Psi_{max}\ + \epsilon \tag{36}$$

where ϵ is a small positive constant. The adaptation technique by Utkin [49] is presented as follows:

$$k(t) = \bar{K}|\eta| + \ \bar{K}_0 \tag{37}$$

Where $\bar{K} > 0, \bar{K}_0 > \ 0$ and η the average of the discontinuous sign(s) obtained through the concept of equivalent control [49].

$$\tau\dot{\eta} + \eta = \ sign(s(x,t)) \tag{38}$$

With $\tau > \ 0$, and $\bar{K}$ is chosen according to Eq. (34). Then there exists a finite time $t_f > 0$ so that the sliding mode is established for all $t \ge t_f$. The main features are that it adjusts the control gain value utilizing the equivalent control concept to evaluate and eliminate uncertainties/perturbation, which decreases the chattering.

B. Second Adaptive Sliding Mode Controller (ASMC2)

This method is a combination of the ASMC1 and another adaptive technique presented in [46] . This method combines the advantages of the first algorithm (ASMC1) and the method mentioned in [46]. This combination is characterized by not requiring prior knowledge of disturbances, which is a positive aspect when it comes to earthquakes. ASMC2 is used by [47] for a case study prototype building under earthquakes, the difference between our approach and that proposed by the researcher in reference [47] is that their method is not suitable for practical implementation due that achieving the aim of (s=0) is unfeasible due to computational sampling and measurement noise. Consequently, we implemented a minor enhancement that was suggested in reference [49] to ensure that the method is feasible for practical application. This method does not require knowledge of the upper bounds of disturbances and uncertainties [49]This increases the design flexibility, given the unexpected intensities of earthquakes. Modified ASMC2 design will be explained as follows:

$$u = -k(t)sign(s) \tag{39}$$

- If $|s(x,t)| > \varepsilon > 0$, $k(t)$ is the solution of

$$\dot{k} = \overline{K_1}.\,|s(x,t)| \tag{40}$$

With $\overline{K_1} > 0$ & $k(0) > 0$

- If $|s(x,t)| \leq \varepsilon, k$ is

$$\begin{gathered} k(t) = \bar{K}.\,|\eta| + \bar{K}_0 \\ \tau\dot{\eta} + \eta = sign(s(x,t)) \end{gathered} \tag{41}$$

Where $\varepsilon > 0$ a small constant. The control law in Eq. (41) is active when $|s(x,t)| > \varepsilon$ the adaptive sliding mode control law (42) works as follows [49] :

- The gain $k(t)$ increases according to the adaptation law (41) until it reaches a value sufficient to counteract the bounded disturbance with unknown limits in Eq. (3). This process continues until the sliding mode is established. The time at which the sliding mode first begins is denoted as t_1.
- When the sliding mode begins i.e. $s(x(t),t) \leq \varepsilon$starting from $t=t_1$, the gain k follows the adaptation law (42). Subsequently, k is adjusted according to Eq. (38), with $\bar{K} = k(t_1)$.This strategy allows the gain to be reduced and then adjusted in response to the current uncertainties or perturbations. Thus, the process will repeat each time |s| exceedsε [20].

ASMC1 and ASMC2 are applied to the system in (3) employing an ATMD in (6) and (7) and then an MRD in Eq (8) to Eq (15).

To avoid chattering phenomena in both controllers caused by the discontinuous signum function (sign), the saturation function [38] will be used instead in Eq. (31) and Eq. (40)

$$sat(s) = \begin{cases} sign(s), & if\,|s| > \varphi \\ \dfrac{s}{\varphi}, & if\,|s| \leq \varphi \end{cases} \tag{42}$$

Where $\varphi$is the boundary layer width. The replacement of the sign with saturation decreases chattering; however, this change resulted in a relative drop in robustness. The accuracy of the saturation decreases relatively, depending upon its boundary layer φ.

IV. Simulation and Result

In this section, two scenarios are presented to evaluate the effectiveness of the control algorithms on a three-story building equipped with dampers. The damper was installed on the top floor, and to test the robustness of the systems used, the building was subjected to seismic conditions of varying intensities. The earthquakes used were the ELCentro1940 and Mexico City earthquakes. In scenario 1 a comparison was made between ASMC1 and ASMC2 using an active damper. After demonstrating the superiority of ASMC2, it was tested under a more intense earthquake, the El Centro1940 earthquake, to compare the active damper and the semi-active damper performances. In scenario 2 a comparison was made between ASMC2 comparing different locations of the MRD under the same seismic conditions. Another comparison was made with a robust controller from a previous study [48] to show the effectiveness of the proposed ASMC. The numerical simulations were conducted in the MATLAB/SIMULINK environment. The building specifications are presented in Table I, while the damper parameters are detailed in Table II.

TABLE I. Parameter of the Building [51]

Parameter	Values	Units
Mass matrix (M)	$\begin{bmatrix} 98.3 & 0 & 0 \\ 0 & 98.3 & 0 \\ 0 & 0 & 98.3 \end{bmatrix}$	Kg
Damping matrix (C)	$\begin{bmatrix} 175 & -50 & 0 \\ -50 & 100 & -50 \\ 0 & -50 & 50 \end{bmatrix}$	Ns/m
Stiffness matrix (K)	$10^5\begin{bmatrix} 12 & -6.84 & 0 \\ -6.84 & 13.7 & -6.84 \\ 0 & -6.84 & 6.84 \end{bmatrix}$	N/m

TABLE II. Parameter of Dampers [51], [60]

Dampers	Parameter	Value
ATMD	m_d	2.89 kg
	c_d	2.37×10^{-3}N. s/m
	k_d	3.84×10^{3}N/m
MRD	c_{0a}, c_{0b}	21$N.s/cm$,3.5$N.s/cm$
	k_0, a	46.9 N/cm, 301
	c_{1a}, c_1	283 $N.s/cm$, 2.95 $N.s/$cm
	r	2
	α_a ,α_b	140 N/cm, 695 $N/$cm
	γ ,β	363 cm^{-2}, 363 cm^{-2}
	η , x_0	190s^{-1}, 0
	v_{max}	2.25volt

A. Scenario I : Analysis of Maximum Structural Responses Using ATMD and MRD

In this study, two adaptive SMC are designed and compared: ASMC1 and ASMC2. The controller parameters are set as $\bar{G}$= [0 0 0 0 0 1], with τ= 0.1 and $\bar{K}_0$= 2, $\overline{K_1}$=300. In this scenario, the ATMD responses are regulated by ASMC1 and ASMC2, under a time scaled Mexico City earthquake, the damper is positioned on the top floor. The aim of this scenario is to evaluate the efficacy of ATMD in mitigating seismic effects governed by the two different algorithms as compared to the open-loop case. The uncontrolled displacement of the three-story scaled structure during the time-scaled Mexico City earthquake is shown in Fig. 3 and Fig. 4. ASMC1 and ASMC2 controlled responses of the three stories under the Mexico City earthquake using ATMD are compared in Fig. 5. and Fig. 6. The result demonstrates that both methodologies exhibit significant improvements when used with the active damper as compared to the uncontrolled case. The second strategy ASMC2 surpasses ASMC1 by achieving greater displacement reduction and less energy consumption. This is confirmed by the statistical results of the comparison of both controllers ASMC1 and ASMC2 presented in Table III and Table IV.

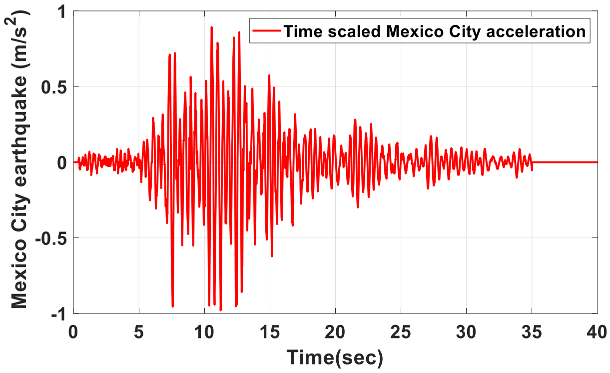

Fig. 3. Mexico City earthquake acceleration

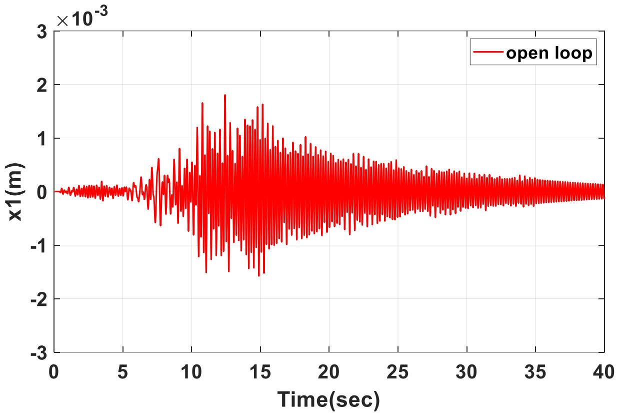

(a)

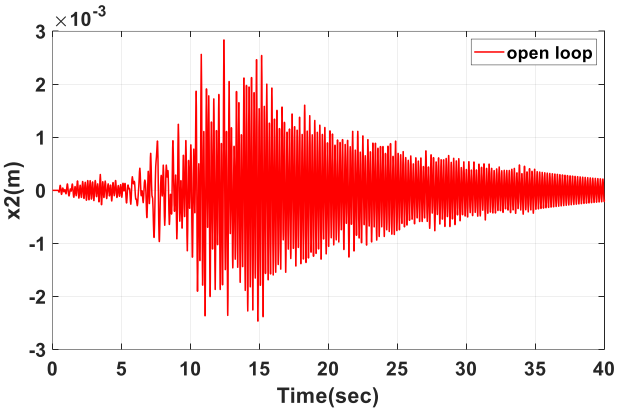

(b)

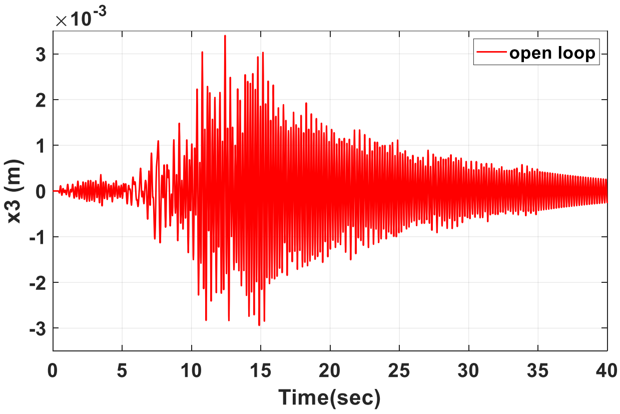

(c)

Fig. 4. Uncontrolled Displacement of three floors (a, b, c) respectively under effect of scaled Mexico City Earthquake

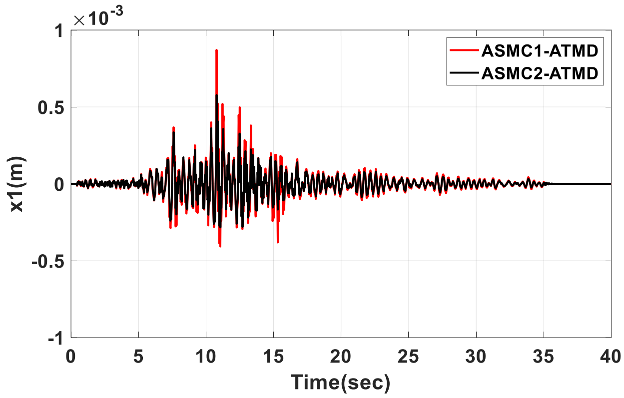

(a)

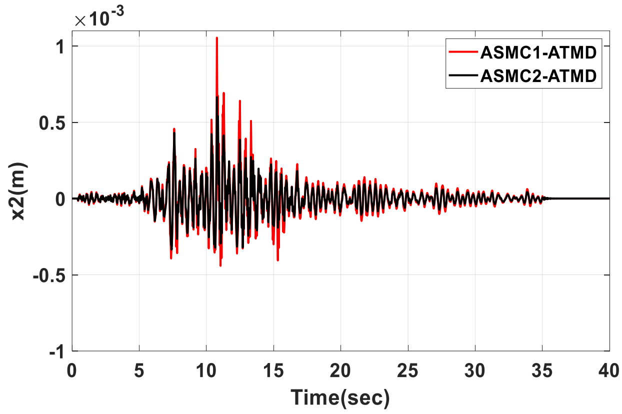

(b)

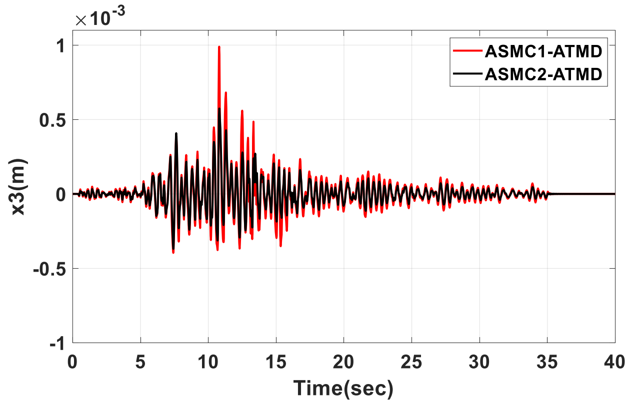

(c)

Fig. 5. Displacement for three floors (a, b, c) respectively under effect of Mexico City earthquake with ATMD controlled by ASMC1and ASMC2

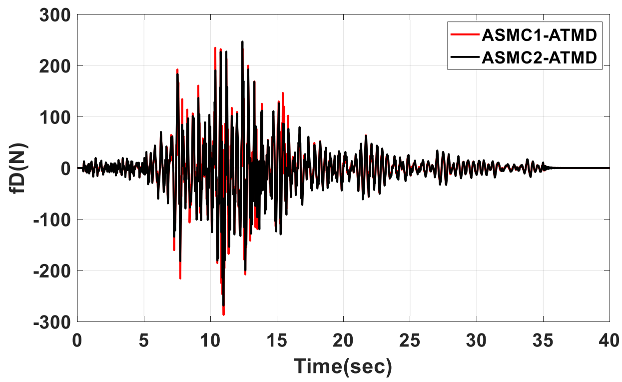

Fig. 6. The control force by ATMD under effect of time scaled Mexico City earthquake

TABLE III. MAXIMUM STRUCTURAL RESPONSES USING ATMD UNDER MEXICO CITY EARTHQUAKE

Outputs	Open loop	Controllers	
		ASMC1	ASMC2
$\lvert x_1\rvert(m)$	0.002	0.00087	0.00057
$\lvert x_2\rvert(m)$	0.003	0.0011	0.00061
$\lvert x_3\rvert(m)$	0.0034	0.0012	0.00066
$f_D(N)$	/	286.98	268.6

TABLE IV. PERFORMANCE SYSTEM WITH ATMD UNDER MEXICO CITY EARTHQUAKE

Outputs	ASMC1-ISE	ASMC2-ISE	ASMC1-ITAE	ASMC2-ITAE
$\lvert x_1\rvert(m)$	0.0000002	0.0000001	0.0018	0.0015
$\lvert x_2\rvert(m)$	0.0000005	0.0000002	0.0026	0.0019
$\lvert x_3\rvert(m)$	0.00000058	0.00000021	0.0028	0.0020

Now, ASMC2 with ATMD is compared to MRD under the El Centro 1940 earthquake, which is three times more intense than the previous earthquake. This comparison aims to identify the most efficient damping device with this control algorithm under different disturbance bounds. Both dampers contributed to reducing the top floor displacement, but the MRD demonstrated a significant improvement of 89.01% compared to ATMD. Additionally, the results showed a notable improvement in energy efficiency, with MRD reducing the consumed force by 19.17% compared to ATMD. These improvements reflect the superior performance of MRD in reducing structural displacement and energy consumption, enhancing its effectiveness in improving the stability of the structure under dynamic influences during the El Centro 1940 earthquake. The simulation results are presented in Fig. 7, Fig. 8, Fig. 9 and Fig. 10. Table V and Table VI present the statistical outcomes of the actuators.

TABLE V. MAXIMUM STRUCTURAL USING ATMD AND MRD UNDER ELCENTRO 1940 EARTHQUAKE

Out put	Open loop	ASMC2-ATMD	ASMC2-MRD
$\lvert x_1\rvert(m)$	0.0055	0.0028	0.0010
$\lvert x_2\rvert(m)$	0.011	0.0038	0.0013
$\lvert x_3\rvert(m)$	0.012	0.0042	0.00132
$f_D(N)$	/	893.89	722.6

TABLE VI. RMS COMPARISON OF ASMC2 WITH ATMD AND MRD UNDER ELCENTRO 1940 EARTHQUAKE

Output	ASMC2-ATMD	ASMC2-MRD
$\lvert x_1\rvert(m)$	0.000314	0.000198
$\lvert x_2\rvert(m)$	0.000427	0.000269
$\lvert x_3\rvert(m)$	0.000475	0.000294
$f_D(N)$	136.563	112.062

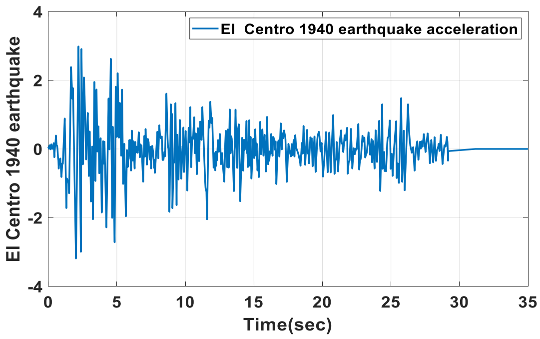

Fig. 7. El Centro 1940 earthquake acceleration

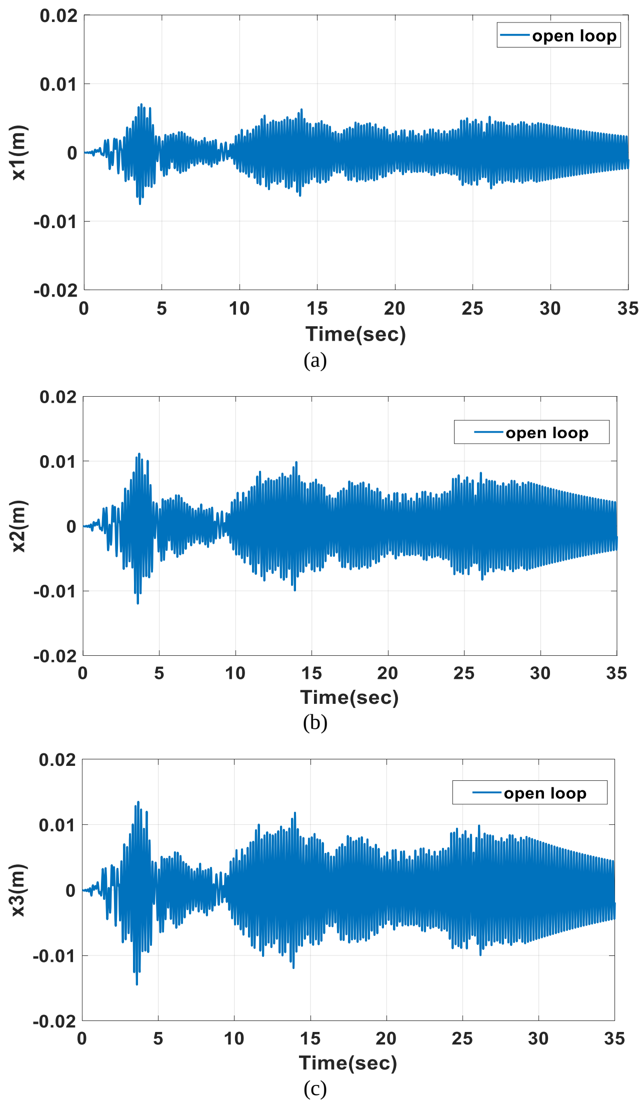

Fig. 8. Uncontrolled Displacement of three floors (a, b, c) respectively under effect of scaled El Centro Earthquake

B. Scenario II: Comparison with Other Studies

To determine the impact of MRD location with ASMC2 on the results and their quality. The previous design of ASMC2 in [47], was with the MRD placed on the ground floor. In this work the proposed MRD location is on the top floor. The results of ASMC2 with MRD in these two different locations are compared in this scenario. This comparison showed that placing the damper on the top floor leads to an improvement in reducing the displacement of all floors relative to the open loop as shown in Table VII using the displacement floor reduction ratio [47] :

$$Rd_r = \frac{|x_i^{max}| - max|x_i|}{|x_i^{max}|} \tag{43}$$

Where *Rdr* is the displacement reduction ratio, x_i is the peak floor displacement, x_i^{max} is the uncontrolled floor peak displacement.

The results showed that placing the damper on the top floor is more effective. Next, ASMC2 with MRD on the top floor will be compared to ISMC with barrier function (ISMCb) designed in [48] under the influence of two different earthquakes: Mexico and El Centro. The aim of this comparison is presented since both controllers do not require the knowledge of disturbance bounds. This will provide an idea of which of the two SMC approaches is more efficient in reducing vibrations and achieving the objectives of this study. When the building was subjected to the Mexico City earthquake, the displacement reduction for first floor was 71.5% and for the second floor was 79.67%, and for the third floor, it was 80.59%. The consumed force was 28.69%. Also, when building is subjected to the El Centro earthquake, the first-floor displacement improved by 81.82% the second-floor displacement improved by 88.18%, and for the third-floor, it was 89.01%. In terms of energy consumption, the improvement was 3.78% as shown in Table VIII. These results confirm the superiority of ASMC2 in enhancing structural performance, reducing vibrations, and minimizing energy consumption.

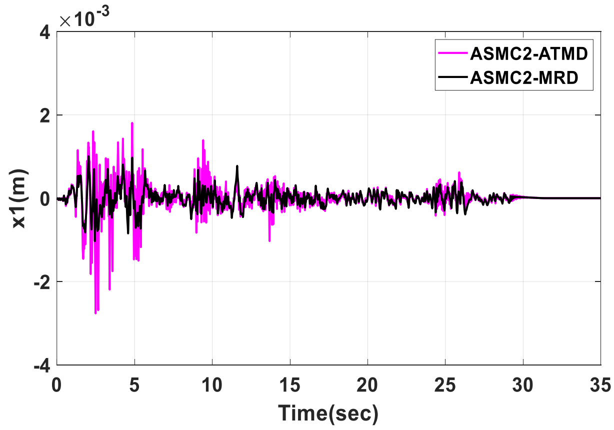

(a)

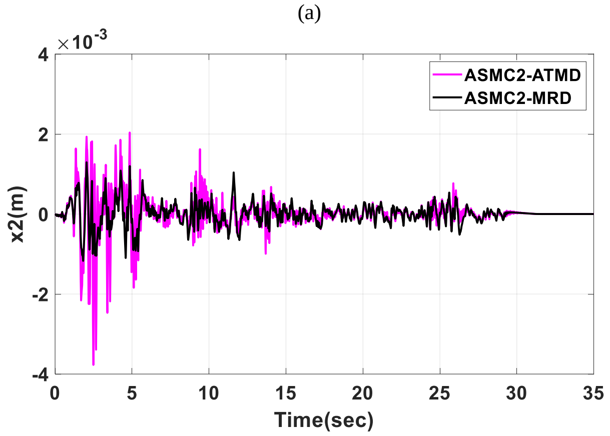

(b)

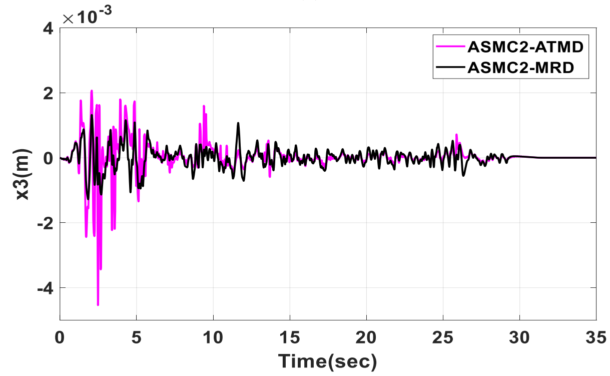

(c)

Fig. 9. Displacement for three floors under effect of El Centro1940 earthquake with ATMD and MRD controlled by ASMC2

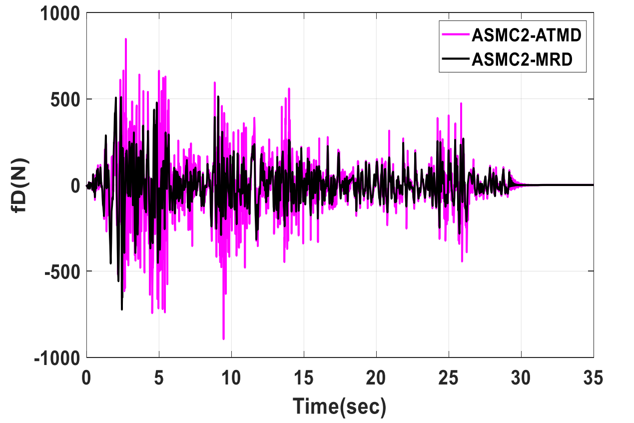

Fig. 10. The control force by ATMD and MRD under effect of El-Centro1940 earthquake

TABLE VII. COMPARISON BETWEEN THE AXIMUM DISPLACEMENT REDUCTION RATIO OF SMC2 AND ASMC [47] DURING THE 1940 EL CENTRO EARTHQUAKE

Rd %	**ASMC** [47]	**ASMC2**
$\lvert x_1 \rvert (m)$	78.05	81.82
$\lvert x_2 \rvert (m)$	73.87	88.18
$\lvert x_3 \rvert (m)$	69.92	89.01

TABLE VIII. COMPARISON OF THE PEAK RESPONSES OF ASMC2 AND ISMCB [48] DURING THE MEXICO CITY AND EL CENTRO EARTHQUAKES

Disturbances	**Out put**	**MRD**	
		ISMCb [48]	**ASMC2**
Mexico City	$\lvert x_1 \rvert (m)$	0.0003	0.0003
	$\lvert x_2 \rvert (m)$	0.00048	0.00046
	$\lvert x_3 \rvert (m)$	0.00058	0.000465
	$f_D(N)$	314	223.92
El Centro 1940	$\lvert x_1 \rvert (m)$	0.00127	0.0010
	$\lvert x_2 \rvert (m)$	0.00197	0.0013
	$\lvert x_3 \rvert (m)$	0.00233	0.00132
	$f_D(N)$	751	722.6

V. CONCLUSION

This study shows the design of two controllers, ASMC1 and ASMC2, for a three-story structure exposed to the Mexico City and El Centro scaled earthquakes. Two dampers were mounted on the top floor, using two different dampers: ATMD and MRD. The ASMC1 controller is distinguished by its ability to adjust the control gain through the equivalent control concept Nonetheless, it needs prior knowledge of the limits of external perturbations. Conversely, the ASMC2 controller does not require this prior knowledge. A numerical simulation was performed to determine the effectiveness of the controllers under two different scenarios. The performance of ASMC1 and ASMC2 was evaluated when combined with ATMD in the initial scenario. The findings indicated that ASMC2 surpassed ASMC1 in minimizing displacement and consuming energy. In the same scenario, to evaluate the effectiveness of ASMC2, a comparison was conducted between ATMD and MRD under a stronger earthquake. The findings demonstrated that MRD with ASMC2 was more effective in minimizing displacement and energy-consumption. The MRD location between the ground and top floors is also studied to confirm that the MRD on the top floor improves the displacement reduction for the same controller. Finaly, ASMC2 results are compared to ISMC with barrier function under the same conditions. This comparison provided a clearer picture of using SMC algorithms which do not need disturbance bounds in their design. This comparison illustrated that ASMC2 have a better statistical result as compared to ISMCb on this kind of systems.

In context of these results, more research is recommended to do practical tests on a scaled structure equipped with MRD to validate the numerical simulations. This implementation may come with some practical issues like the number of sensors and dampers and the related cost and maintenance.

REFERENCES

[1] G. Chen, Y. Wu, M. Xia, and Z. Li, "Focal mechanics and disaster characteristics of the 2024 M 7.6 Noto Peninsula Earthquake, Japan," *Frontiers of Structural and Civil Engineering*, vol. 18, no. 9, pp. 1378–1387, 2024.

[2] M. Shahi, M. R. Sohrabi, and S. Etedali, "Seismic control of high-rise buildings equipped with ATMD including soil-structure interaction effects," *Journal of Earthquake and Tsunami*, vol. 12, no. 03, p. 1850010, 2018.

[3] G. Bekdaş, A. E. Kayabekir, S. M. Nigdeli, and Y. C. Toklu, "Tranfer function amplitude minimization for structures with tuned mass dampers considering soil-structure interaction," *Soil Dynamics and Earthquake Engineering*, vol. 116, pp. 552–562, 2019.

[4] H. Li, M. Askari, J. Li, Y. Li, and Y. Yu, "A novel structural seismic protection system with negative stiffness and controllable damping," *Structural Control and Health Monitoring*, vol. 28, no. 10, p. e2810, 2021.

[5] L. Fali, K. Zizouni, A. Saidi, T. Ghomri, I. K. Bousserhane, and M. Djermane, "Structural vibration control in excited structures: history and prospects," *Journal of Vibration Engineering & Technologies*, vol. 11, no. 3, pp. 1287–1308, 2023.

[6] G. Bekdaş and S. M. Nigdeli, "Metaheuristic based optimization of tuned mass dampers under earthquake excitation by considering soil-structure interaction," *Soil Dynamics and Earthquake Engineering*, vol. 92, pp. 443–461, 2017.

[7] M. Khatibinia, M. Mahmoudi, and H. Eliasi, "Optimal sliding mode control for seismic control of buildings equipped with ATMD," *International Journal of Optimization in Civil Engineering*, vol. 10, no. 1, pp. 1–15, 2020.

[8] J. C. Li, Y. Li, M. Askari, and Q. P. Ha, "Future intelligent civil structures: Challenges and opportunities," *31st International Symposium on Automation and Robotics in Construction and Mining, ISARC 2014-Proceedings*, 2014.

[9] A. Sivakumar, G. Chandrasekaran, and C. A. Cáceres, "Modeling and active vibration suppression of dynamical systems: a survey," *Journal of Science and Engineering*, vol. 7, no. 1, pp. 50–71, 2016.

[10] K. Takin, R. Doroudi, and S. Doroudi, "Vibration control of structure by optimising the placement of semi-active dampers and fuzzy logic controllers," *Australian Journal of Structural Engineering*, vol. 22, no. 3, pp. 222–235, 2021.

[11] Z. Lu, S. F. Masri, and X. Lu, *Particle damping technology based structural control*. Springer, 2020.

[12] S. Ulusoy, S. M. Nigdeli, and G. Bekdaş, "Novel metaheuristic-based tuning of PID controllers for seismic structures and verification of robustness," *Journal of Building Engineering*, vol. 33, p. 101647, 2021.

[13] S. M. Nigdeli and G. Bekdaş, "Optimum tuned mass damper design in frequency domain for structures," *KSCE journal of civil engineering*, vol. 21, pp. 912–922, 2017.

[14] A.-A. Zamani, S. Tavakoli, S. Etedali, and J. Sadeghi, "Adaptive fractional order fuzzy proportional–integral–derivative control of smart base-isolated structures equipped with magnetorheological dampers," *Journal of Intelligent Material Systems and Structures*, vol. 29, no. 5, pp. 830–844, 2018.

[15] A. H. Heidari, S. Etedali, and M. R. Javaheri-Tafti, "A hybrid LQR-PID control design for seismic control of buildings equipped with ATMD," *Frontiers of Structural and Civil Engineering*, vol. 12, pp. 44–57, 2018.

[16] M. Soleymani and M. Khodadadi, "Adaptive fuzzy controller for active tuned mass damper of a benchmark tall building subjected to seismic and wind loads," *The Structural Design of Tall and Special Buildings*, vol. 23, no. 10, pp. 781–800, 2014.

[17] C. M. Moutinhó, A. Cunha, and E. Caetano, "Implementation of an Active Mass Driver for Increasing Damping Ratios of the Laboratorial Model of a Building," *Journal of Theoretical and Applied Mechanics*, vol. 49, no. 3, pp. 791-806, 2011.

[18] K.-C. Lu, C.-H. Loh, J. N. Yang, and P.-Y. Lin, "Decentralized sliding mode control of a building using MR dampers," *Smart Materials and Structures*, vol. 17, no. 5, p. 055006, 2008.

[19] Y. Li, J. Li, T. Tian, and W. Li, "A highly adjustable magnetorheological elastomer base isolator for applications of real-time adaptive control," *Smart Materials and Structures*, vol. 22, no. 9, p. 095020, 2013.

[20] Y. Chae, J. M. Ricles, and R. Sause, "Modeling of a large-scale magneto-rheological damper for seismic hazard mitigation. Part I: Passive mode," *Earthquake Engineering Struct Dynamics*, vol. 42, no. 5, pp. 669–685, 2013.

[21] Y. Li and J. Li, "A highly adjustable base isolator utilizing magnetorheological elastomer: experimental testing and modeling," *Journal of Vibration and Acoustics*, vol. 137, no. 1, p. 011009, 2015.

[22] Y. Ding, L. Zhang, H.-T. Zhu, and Z.-X. Li, "A new magnetorheological damper for seismic control," *Smart Materials and Structures*, vol. 22, no. 11, p. 115003, 2013.

[23] A. N. Vargas, J. G. Raminelli, M. A. F. Montezuma, A. A. Cavalini Junior, R. Breganon, and C. F. Caruntu, "Shaking Table Attached to Magnetorheological Damper: Simulation and Experiments for Structural Engineering," *Sensors*, vol. 22, no. 10, p. 3644, 2022.

[24] A. N. Vargas, J. G. Raminelli, and M. A. F. Montezuma, "Cavalini Junior, AA; Breganon, R.; Caruntu, CF Shaking Table Attached to Magnetorheological Damper: Simulation and Experiments for Structural Engineering," *Sensors*, vol. 22, no. 10, p. 3644, 2022.

[25] M. Basili and M. De Angelis, "Vibration analysis and models of adjacent structures controlled by magnetorheological dampers," *Shock and Vibration*, vol. 2017, no. 1, p. 9596382, 2017.

[26] S. Mohammadyzadeh, A. Mojtahedi, J. Katebi, H. Hokmabady, and F. Hosseinlou, "Semi-active Control of an Offshore Platform Using Updated Numerical Model and Experimental Laser Doppler Vibrometer Data," *International Journal of Coastal, Offshore and Environmental Engineering*, vol. 7, no. 1, pp. 23–33, 2022.

[27] M. F. Farzam, M. M. Safakhanehb, and H. Ahmadia, "Advanced Vibration Control of the Resalat Offshore Jacket Platform Under Seismic Excitations: A Compara-tive Study of Active and Semi-Active Dampers," *The 14th International Conference on Acoustics & Vibration (ISAV2024)*, pp. 1-8, 2024.

[28] Z. R. Wani, M. Tantray, and E. N. Farsangi, "Adaptive System Supervising the Response Control for Smart Structures," *Automation in Construction toward Resilience, CRC Press*, pp. 277–316, 2023.

[29] X. Liang, L. Cheng, T. Liu, and J. Du, "Nonlinear dynamic analysis of the bridge bearing and genetic algorithm–based optimization for seismic mitigation," *Advances in Structural Engineering*, vol. 23, no. 12, pp. 2539–2556, 2020.

[30] S. Jin *et al*., "Development of a semi-active MR inerter for seismic protection of civil structures," *Journal of Intelligent Material Systems and Structures*, vol. 35, no. 15, pp. 1231–1244, 2024.

[31] M. Morales-Beltran and J. Paul, "Active and semi-active strategies to control building structures under large earthquake motion," *Journal of Earthquake Engineering*, vol. 19, no. 7, pp. 1086–1111, 2015.

[32] H.-N. Feng, B.-L. Zhang, Y.-D. Zhao, H. Ma, H. Su, and J. Li, "Vibration control of network-based offshore structures subject to earthquakes," *Transactions of the Institute of Measurement and Control*, vol. 44, no. 4, pp. 861–870, 2022.

[33] K. Ghaedi, Z. Ibrahim, H. Adeli, and A. Javanmardi, "Invited Review: Recent developments in vibration control of building and bridge structures," *Journal of Vibroengineering*, vol. 19, no. 5, pp. 3564–3580, 2017.

[34] K. Takin, R. Doroudi, and S. Doroudi, "Vibration control of structure by optimising the placement of semi-active dampers and fuzzy logic controllers," *Australian Journal of Structural Engineering*, vol. 22, no. 3, pp. 222–235, 2021.

[35] T. K. Dhiman, “Advanced Control Techniques for Active Vibration Control of Structures,” *NeuroQuantology*, vol. 20, no. 8, p. 10482, 2022.

[36] K. Ghaedi, Z. Ibrahim, A. Javanmardi, and R. Rupakhety, “Experimental study of a new bar damper device for vibration control of structures subjected to earthquake loads,” *Journal of Earthquake Engineering*, vol. 25, no. 2, pp. 300–318, 2021.

[37] P. Endla, A. Nainwal, M. S. Al Ansari, M. N. Alemayehu, and N. A. Upadhye, “Structural Engineering Optimization Techniques for Earthquake-Resilient Buildings,” *Structural Engineering Optimization Techniques for Earthquake-Resilient Buildings*, 2024.

[38] A. J. Humaidi, M. E. Sadiq, A. I. Abdulkareem, I. K. Ibraheem, and A. T. Azar, “Adaptive backstepping sliding mode control design for vibration suppression of earth-quaked building supported by magneto-rheological damper,” *Journal of Low Frequency Noise, Vibration and Active Control*, vol. 41, no. 2, pp. 768–783, 2022.

[39] X. Yan, Z. D. Xu, and Q. X. Shi, “Fuzzy neural network control algorithm for asymmetric building structure with active tuned mass damper,” *JVC/Journal of Vibration and Control*, vol. 26, no. 21–22, pp. 2037–2049, 2020.

[40] M. Khatibinia, M. Mahmoudi, H. Eliasi, M. Khatibinia, M. Mahmoudi, and H. Eliasi, “Optimal Sliding Mode Control for Seismic Control of Buildings Equipped With ATMD,” *International Journal of Optimization in Civil Engineering*, 2020.

[41] M. Wasilewski, D. Pisarski, and C. I. Bajer, “Adaptive optimal control for seismically excited structures,” *Automation in Construction*, vol. 106, p. 102885, 2019.

[42] L. Li, N. Wang, and H. Qin, “Adaptive model reference sliding mode control of structural nonlinear vibration,” *Shock and Vibration*, vol. 2019, 2019.

[43] Kavyashree, H. M. Jagadisha, V. S. Rao, and Bhagyashree, “Classical PID controller for semi-active vibration control of seismically excited structure using magneto-rheological damper,” *Global Challenges in Energy and Environment: Select Proceedings of ICEE 2018*, pp. 201–210, 2020.

[44] K. Zizouni, I. K. Bousserhane, A. Hamouine, and L. Fali, “MR damper-LQR control for earthquake vibration mitigation,” *International Journal of Civil Engineering and Technology*, vol. 8, no. 11, pp. 201–207, 2017.

[45] K. Zizouni, L. Fali, Y. Sadek, and I. K. Bousserhane, “Neural network control for earthquake structural vibration reduction using MRD,” *Frontiers of Structural and Civil Engineering*, vol. 13, no. 5, pp. 1171–1182, 2019.

[46] A. Saidi, K. Zizouni, B. Kadri, L. Fali, and I. K. Bousserhane, “Adaptive sliding mode control for semi-active structural vibration control,” *Studies in Informatics and Control*, vol. 28, no. 4, pp. 371–380, 2019.

[47] K. Zizouni, A. Saidi, L. Fali, I. K. Bousserhane, and M. Djermane, “Adaptive sliding-mode control for improved vibration mitigation in civil engineering structures,” *Mechanical Sciences*, vol. 13, no. 2, pp. 899–908, 2022.

[48] S. S. Husain and T. MohammadRidha, “Integral Sliding Mode Control for Seismic Effect Regulation on Buildings Using ATMD and MRD,” *Journal Europeen des Systemes Automatises*, vol. 55, no. 4, pp. 541–548, 2022.

[49] F. Plestan, Y. Shtessel, V. Bregeault, and A. Poznyak, “New methodologies for adaptive sliding mode control,” *International Journal of Control*, vol. 83, no. 9, pp. 1907–1919, 2010.

[50] H. Lee and V. I. Utkin, “Chattering suppression methods in sliding mode control systems,” *Annual Reviews in Control*, vol. 31, no. 2, pp. 179–188, 2007.

[51] S. S. Husain and T. MohammadRidha, “Design of Integral Sliding Mode Control for Seismic Effect Regulation on Buildings with Unmatched Disturbance,” *Mathematical Modelling of Engineering Problems*, vol. 9, no. 4, pp. 1123–1130, 2022.

[52] O. Yoshida and S. J. Dyke, “Seismic control of a nonlinear benchmark building using smart dampers,” *Journal of Engineering Mechanics*, vol. 130, no. 4, pp. 386–392, 2004.

[53] J. Wang, Y. Liu, Z. Qin, L. Ma, and F. Chu, “Dynamic performance of a novel integral magnetorheological damper-rotor system,” *Mechanical Systems and Signal Processing*, vol. 172, p. 109004, 2022.

[54] A. E. Kayabekir, G. Bekdaş, S. M. Nigdeli, and Z. W. Geem, “Optimum design of PID controlled active tuned mass damper via modified harmony search,” *Applied Sciences*, vol. 10, no. 8, p. 2976, 2020.

[55] S. S. Husain and T. MohammadRidha, “Integral Sliding Mode Control for Seismic Effect Regulation on Buildings Using ATMD and MRD,” *Journal Europeen des Systemes Automatises*, vol. 55, no. 4, pp. 541–548, 2022.

[56] L. Fali, M. Djermane, K. Zizouni, and Y. Sadek, “Adaptive sliding mode vibrations control for civil engineering earthquake excited structures,” *International Journal of Dynamics and Control*, vol. 7, no. 3, pp. 955–965, 2019.

[57] D. A. Pohoryles and P. Duffour, “Adaptive control of structures under dynamic excitation using magnetorheological dampers: An improved clipped-optimal control algorithm,” *JVC/Journal of Vibration and Control*, vol. 21, no. 13, pp. 2569–2582, 2015.

[58] A. J. Humaidi, S. Hasan, and A. A. Al-Jodah, “Design of second order sliding mode for glucose regulation systems with disturbance,” *International Journal of Engineering & Technology*, vol. 7, no. 2.28, pp. 243–247, 2018.

[59] A. H. Hameed, A. Q. Al-Dujaili, A. J. Humaidi, and H. A. Hussein, “Design of terminal sliding position control for electronic throttle valve system: A performance comparative study,” *International review of automatic control*, vol. 12, no. 5, pp. 251–260, 2019.

[60] K. Zizouni, L. Fali, I. Khalil Bousserhane, and Y. Sadek, “Active Mass Damper Vibrations Control Under Earthquake Loads,” *International Journal of Advances in Mechanical and Civil Engineering*, vol. 7, no. 2, pp. 26-30, 2020.

[61] A. K. Hamoudi and L. T. Rasheed, “Design of an Adaptive Integral Sliding Mode Controller for Position Control of Electronic Throttle Valve,” *Journal Europeen des Systemes Automatises*, vol. 57, no. 3, pp. 729–735, 2024.

[62] T. MohammadRidha and S. A. Al-Samarraie, “A Barrier Function-Based Integral Sliding Mode Control of Heart Rate During Treadmill Exercise*,” Mathematical Modelling of Engineering Problems*, vol. 10, no. 1, pp. 179-188, 2023.

[63] L. Li, N. Wang, and H. Qin, “Adaptive model reference sliding mode control of structural nonlinear vibration,” *Shock and Vibration*, vol. 2019, no. 1, p. 3612516, 2019.

[64] P.-C. Chen and C.-T. Lai, “Advanced control strategy for floor response replication of high-rise buildings subjected to earthquakes,” *Journal of Earthquake Engineering*, vol. 26, no. 3, pp. 1228–1252, 2022.